IEEE Access
Multidisciplinary | Rapid Review | Open Access Journal

SPECIAL SECTION ON WEARABLE AND IMPLANTABLE DEVICES AND SYSTEMS

Received June 12, 2018, accepted July 17, 2018, date of publication July 25, 2018, date of current version August 15, 2018.

Digital Object Identifier 10.1109/ACCESS.2018.2859383

WE-Safe: A Self-Powered Wearable IoT Sensor Network for Safety Applications Based on LoRa

FAN WU, (Student Member, IEEE), JEAN-MICHEL REDOUTÉ, (Senior Member, IEEE), AND MEHMET RASIT YUCE, (Senior Member, IEEE)

Department of Electrical and Computer Systems Engineering, Monash University, Melbourne, VIC 3800, Australia

Corresponding author: Mehmet Rasit Yuce (mehmet.yuce@monash.edu)

This work was supported by the Monash University's Faculty of Engineering Seed Funding. The work of M. R. Yuce was supported by the Australian Research Council Future Fellowships under Grant FT130100430.

ABSTRACT Poor environmental conditions can lead to severe health problems. It is essential to develop effective, reliable, and fast response systems for people working in hazardous environments. This paper presents a wearable Internet of Things sensor network aimed at monitoring harmful environmental conditions for safety applications via a Lora wireless network. The proposed sensor node, called the WE-Safe node, is based on a customized sensor node, which is self-powered, low-power, and supports multiple environmental sensors. Environmental data is monitored by the sensor node in real-time and transmitted to a remote cloud server. The data can be displayed to users through a web-based application located on the cloud server and the device will alert the user via a mobile application when an emergency condition is detected. The experimental results indicate that the presented safety monitoring network works reliably using energy harvesting.

INDEX TERMS Internet of Things, wearable sensor network, safety application, environmental monitoring, energy harvesting, LoRa-based sensor node.

I. INTRODUCTION

Wearable sensor nodes are generally deployed in wireless body area networks (WBAN) to monitor physiological parameters, such as body skin temperature [1], photoplethysmogram (PPG), or electrocardiogram (ECG) [2]–[4]. In addition to medical signals, they can be deployed to monitor environmental conditions around the human body as well, such as in the safety application [5], and environmental monitoring applications [6], [7].

Such a wearable sensor system can also provide invaluable and useful information about the environmental impact on subjects' health. People can also gain a deeper understanding of their local micro-environment [8]. A wearable system is not only limited to personal use, it can also be installed on a bicycle, car, and animal to form a wearable or mobile wireless sensor networks. For example, in [9], a mobile node is installed on bicycle for environmental monitoring.

The power supply of sensor nodes is a major challenge for autonomous wearable sensor nodes, because many devices require regular battery replacement or charging. To allow long-term operation and minimize the human interaction of the wearable sensor node, the system has to be low power consumption and adopt energy harvesting [4], [10]. There is a need for an efficient and effective energy harvesting module, which can address this power supply issue. There are several options for energy sources, such as thermoelectric, piezoelectric, micro-magneto-electric, or photoelectric harvesting techniques [11]. Solar energy provides the highest power density among these with high output voltages [12], [13]. The drawback is that the solar energy will disappear at night and this should be considered in the power management unit of a sensor node.

This paper presents a self-powered wearable IoT sensor network, named as WE-Safe IoT project, for safety environmental monitoring. Each sensor node consists of a micro-power manager, a sensing unit, and a wireless module. The micro-power manager is designed to harvest energy both indoors and outdoors to enable a continuous energy supply for the sensor node. The total sensor node is low power consuming 5.6 μA in sleep mode. The data collected is transmitted to a gateway via a long-range LoRa wireless technology. The complete system architecture is shown in Fig. 1. The proposed network provides an effective solution for safety environmental applications. The remainder of this paper is organized as follows: Section 2 discusses related work, Section 3 outlines the system implementation;

2169-3536 © 2018 IEEE. Translations and content mining are permitted for academic research only.
Personal use is also permitted, but republication/redistribution requires IEEE permission.
See http://www.ieee.org/publications_standards/publications/rights/index.html for more information.

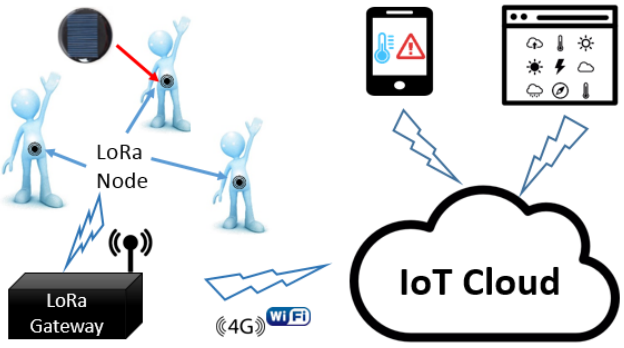

FIGURE 1. The network diagram of the proposed wearable sensor network.

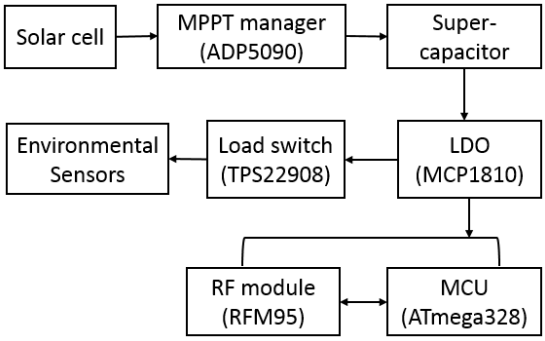

FIGURE 2. The block diagram of the wearable node.

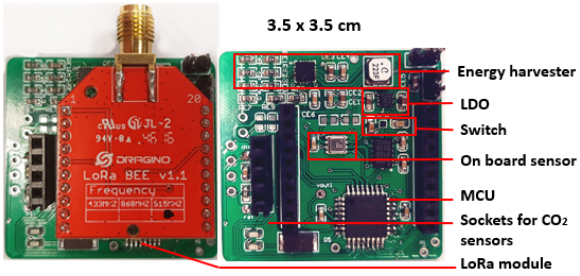

FIGURE 3. Hardware implementation of WE-Safe IoT sensor node.

Section 4 discusses the experimental results, and a brief conclusion is given in Section 5.

II. RELATED WORK

The work reported in [5] presents a wearable safety application, which allows early detection of hazardous situations for exposed workers. It can detect CO_2, temperature and relative humidity. The wearable system is based on the XBee DigiMesh module and is powered by a (800 mAh) Lithium Polymer battery.

The work described in [6] presents a wearable environmental sensor network for urban environment monitoring. It has seven environmental sensors including infrared temperature sensor, atmospheric pressure, accelerometer, temperature, humidity, ambient light, and inertial measurement unit (IMU). The rechargeable battery provides the power and can last for 7 days. Wireless connectivity is achieved by a on-board Wi-Fi module.

Reference [7] presents a low power and wearable sensor network measuring CO_2 concentration, the Earth's magnetic field, temperature and relative humidity monitoring. The sensor node is based on Bluetooth wireless node and powered by a rechargeable Li-ion battery. However, wearable nodes still require regularly recharging the battery, which is inconvenient.

The work reported in [8] presents a wearable and wireless system for toxic environmental volatile organic compounds (VOC), temperature, and relative humidity monitoring. A Bluetooth interface is used to transmit the data from the sensor device to a mobile phone.

In work [9], a mobile sensor node is installed on a bicycle for environmental monitoring. The proposed system can monitor air pollutants including O_2 and PM_{10}. The wireless network utilize a ZigBee module. In continuous monitoring mode, the total run time can be up to 60 h.

III. WE-SAFE IMPLEMENTATION

In order to design the hardware and software for a wearable sensor network system, the environmental sensors' selection and the networking protocol need to be carefully considered upfront. In this work, low power electronics and solar energy harvesting techniques are deployed to enable a continuous power supply for the sensor node. The wearable sensor network is based on the long range LoRa wireless technology. Fig. 2 presents the block diagram of the wearable node. Fig. 3 shows the picture of the wearable node. Specifications of the WE-Safe IoT sensor node are shown in Table. 1.

TABLE 1. Specifications of WE-Safe IoT sensor nodes.

Component	Part	Specification
Power source	Round solar panel	Radius: 3 cm
MPPT controller	ADP5090	Input: 80 mV to 3.3 V
Energy storage	Super-capacitor	12.5 F
LDO	MCP1810	Input: 3.68 to 5.5 V
QOD switch	TPS22908	Input: 1 to 3.6 V
Wireless	RFM95	LoRa
MCU	ATmega328p	3.3V @ 8 MHz
Temperature	BME680	-40 to +85 °C
Humidity	BME680	0 to 100 %RH
UV index	SI1145	1 to 11+ Index
CO_2	COZIR-GC0012	0 to 10,000 ppm

Each wearable sensor node consists of three major sections: A. Sensor node, B. Wireless network, and C. Micro-power manager. These will be discussed in detail here below.

A. SENSOR NODE

The ATmega328p from Atmel Corporation is selected as the micro-controller (MCU) in this work [14]. It collects the data

from different sensors and interfaces with the LoRa chip. It also controls the low power function of the entire wearable node. The MCU has low power consumption (4.4 μA in sleep mode), is low cost, and has high performance features. It has six 10-bit analog-to-digital converters (ADC) and 14 digital pins, which can support various functions required by the sensor board. The nominal voltage for the MCU is 3.3V when the clock speed is 8 MHz.

Temperature and relative humidity are acquired by using a BME680 sensor manufactured by Bosch-sensortec [15]. The BME680 is a low-power sensor consuming only 2.1 μA at 1 Hz. It consumes only 0.15 μA in sleep mode. It features accuracy of $\pm$ 0.5 °C for the temperature and $\pm$ 3% for the relative humidity. This sensor communicates with the MCU via an I2C interface.

The CO_2 sensor selected in this study is the ultra low power COZIR-CO_2 sensor manufactured by CO2 Meter [14], [16]. It consumes little power (3.5 mW) and provides high accuracy ($\pm$ 50 ppm). The sensor requires a short warm-up period, which ranges from 1.2 s to 32 s depending on the digital filter settings. In this work, the filter value is set to 8 and it requires 9 s warm-up time. The sensor can measure CO_2 concentration from 0 to 10,000 ppm, which can be used in both indoor and outdoor measurements.

SI1145 from Silicon Labs is chosen as the UV sensor [17]. It measures the UV index, proximity, and ambient light sensor. It is also a low power sensor consuming less than 500 nA in standby mode and 9 μA on average while measuring. The sensor communicates with the MCU via I2C interface.

B. WIRELESS TRANSMISSION

To provide a long range, low power and low cost solution for the wearable network, the wireless transmission of WE-Safe is based on the LoRa technology. LoRa is a proprietary spread spectrum modulation technique developed by Semtech [18].

In this work, the RFM95 module from Hope Microelectronics [19] is selected as the LoRa module. The module is a low power and long range transceiver module, which provides high interference immunity whilst minimizing current consumption. It has a high sensitivity which is -148 dBm. The receive current is very low and is only 10.3 mA. The module operates in Industrial, Scientific, and Medical (ISM) radio band at 915 MHz in Australia. RFM95's operating voltage is from 1.8 to 3.7 V and the operating temperature is from -20 to $+70$ °C.

The sleep current of the RFM95 is only 0.2 μA. The LoRa module communicates with MCU via Serial Peripheral Interface bus (SPI). RadioHead [20] Packet Radio library is used to communicate between LoRa and MCU. The RF module is LoRa BEE v1.1 in XBee layout from Dragino as shown in Fig. 3. Some important characteristics are listed below:

- Operating temperature range: -20 to $+70$ °C
- Operating voltage: 1.8 to 3.7 V
- Receive current: 10.3 mA
- Sleep current: 0.2 μA
- Transmit current: 20 mA to 120 mA
- Sensitivity: -148 dBm
- Operating frequency: ISM 915 MHz

C. MICRO-POWER MANAGER AND POWER REQUIREMENT

1) MICRO-POWER MANAGER

The power management system includes a round solar panel (radius: 3cm), an ultra-low power MPPT controller (ADP5090 from Analog Devices), a 12.5 F supercapacitor, a low dropout voltage regulator (MCP1810 from Microchip Technology), and a quick-output discharge switch (TPS22908 from Texas Instruments). All these devices are low power and can be paired together for a complete ultra-low power solution.

ADP5090 is used to regulate the solar energy and store the energy into the super-capacitor. This device is an ultra-low power boost regulator with a very low input voltage (80 mV) [21]. This boost converter has a maximum power point tracking (MPPT) function, which is achieved by sampling the open voltage of the solar panel every 19 sec and then track the solar energy at a programmable MPPT ratio. The chip also has a programmable voltage monitor that can support charging and prevent overcharging or over-discharging for battery.

MCP1810 is a ultra-low power voltage regulator. It consumes only 20 nA quiescent current while delivering 150 mA, and regulates the output voltage to a constant 3.3 V for the entire circuit. The maximum dropout voltage is 380 mV [22].

TPS22908 is a low on-resistance (28 mΩ) load switch with the quick output discharge (QOD) function [23]. The switch can quickly discharge the output pin of the switch when the devices are disabled instead of leaving the electronic devices in a floating state. The switch is controlled by a digital pin of MCU. The maximum quiescent current of the switch is only 1 μA.

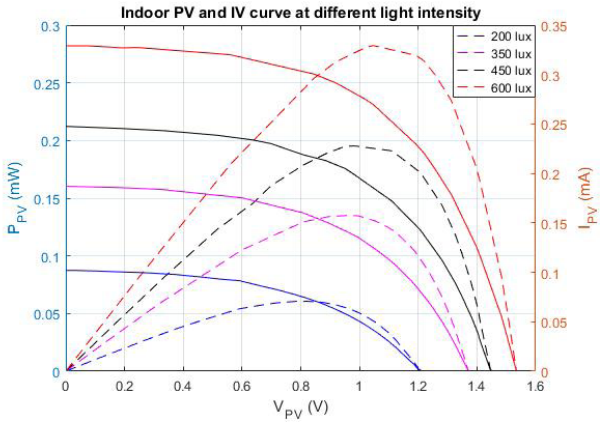

FIGURE 4. The solar panel's characteristic at indoor ambient light condition (IV: solid lines; PV: dashed lines).

Fig. 4 shows the solar panel's characteristic under different room light intensities. The light intensity is ranging from 200 lux to 600 lux. It can be seen that, at 200 lux, the solar

panel can output maximum 0.13 mW at 0.85 V while the open voltage of the solar panel is 1.3 V. The MPPT ratio is 0.85 / 1.3 = 0.66. At 600 lux, the solar panel can output maximum 0.7 mW power at 1.243 V while the open voltage of the solar panel is 1.8 V. The MPPT ratio is 1.243 / 1.8 = 0.7.

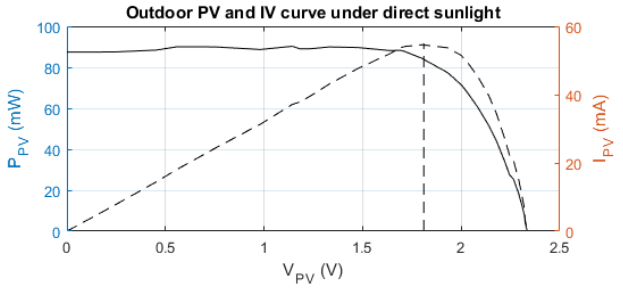

FIGURE 5. The solar panel's characteristic under direct sunlight (IV: solid lines; PV: dashed lines).

Fig. 5 shows the characteristic of the solar panel outdoors and in direct sunlight. Compared to the indoor IV and PV curves, the output power of the solar panel outdoors is much higher. Exposed to direct sunlight, the maximum power can reach 90 mW at 1.8 V.

2) POWER REQUIREMENTS

There are four modes of operation of the WE-Safe IoT sensor nodes: sense mode, transmit mode, idle mode, and sleep mode.

The supply voltage for the entire node is 3.3 V. It requires 5.7 mA when the sensor node is in sense mode, and 48 mA current when the LoRa module is transmitting, 4 mA in idle mode, and 5.6 μA in sleep mode. The power consumption of the wearable node in different modes is tabulated in Table 2.

TABLE 2. Power requirements in different modes.

Stage	Current (mA)	Power (mW)	Duration (s)	Mode
1	5.7	18.81	9	Sense
2	48	158.4	0.05	Transmit
3	4	43.56	0.05	Idle
4	0.0056	0.018	T	Sleep

The programmable MPPT ratio of ADP5090 is configured to be 70 % of the open voltage of the solar panel. Because the LDO minimum input voltage needs to be higher than 3.3 V + 0.38 V = 3.68 V, the termination charging voltage for the super-capacitor is configured to be 4 V. In order to prevent the battery from over-discharging, the shutdown voltage for the super-capacitor is configured to be 3 V.

To minimize the power consumption for the WE-Safe node, all sensors are turned off via the switch (TPS22908) in sleep mode after their readings are measured. Therefore, when calculating the total sleep current, only the power consumption for the MCU, LoRa module, and micro-power manager are considered. While in the sleep mode, the MCU consumes approximately 4.4 μA, the RF module consumes 0.2 μA, the LDO consumes 20 nA, and the switch consumes 1 μA. In total, the sensor node consumes 5.6 μA in sleep mode.

Sense mode is when the sensor node wakes up and measures the environmental conditions. It lasts 9 s and consumes 5.7 mA during that time. In transmit mode, the sensor node consumes 48 mA and lasts for 0.05 s. In idle mode, the LoRa module and sensors are turned off while the MCU still remains awake to measure the current energy level and calculate the sleep time for next duty cycle. The sensor node consumes 4 mA for 0.05 s. The average current in these three modes is equal to (5.7 mA * 9 s+48 mA * 0.05 s +4 mA * 0.05 s)/9.1 s = 53.9 / 9.1 = 5.92 mA.

3) DUTY-CYCLE ADJUSTMENT

In order to accurately measure the environmental conditions, the total times for the duration of the sense, transmit and idle modes are fixed.

However, the sleep time can be dynamically adjusted according to the energy level of the super-capacitor and the current light intensity. Therefore, the duty-cycle can change every period.

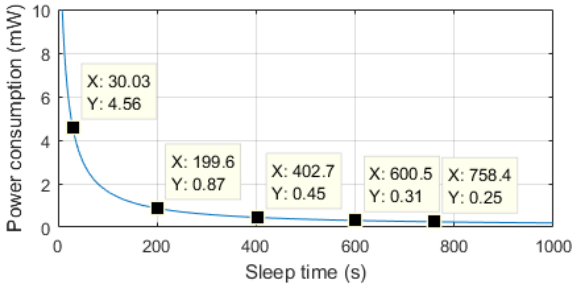

FIGURE 6. Power consumption vs sleep time (s).

Equation 1 represents the power consumption according to different sleep times T. By increasing T, the power consumption will be reduced as shown in Fig. 6. The sleep time required to achieve a perfect energy balance can be derived from Equation 1 and is shown in Equation 2.

$$\begin{aligned} P &= V * I \\ &= 3.3 * (53.9 + 0.0056 * T)/(T + 9.1)\, mW \qquad (1) \\ T &= (177.87 - 9.1 * P)/(P - 0.01848)\, mW \qquad (2) \end{aligned}$$

The solar panel's cell voltage is taken by MCU each duty cycle. The power extracted from the solar panel can be predicted based on the cell voltage. For example, when the cell voltage is recorded at 1 V, it means the energy harvester is harvesting energy at the current maximum power point under the current indoor light intensity 600 lux. According to Fig. 6, the maximum power at this point is 0.28 mW. The sleep time will be automatically adjusted to be greater than 760 s in order to achieve energy balance.

D. SOFTWARE DESIGN FOR THE WEARABLE NETWORK

The wearable nodes are programmed to wake up every minute to track the changing environmental conditions by default. They can also be programmed to run in continuous monitoring mode, which is able to update the environmental data according to users' requirements. When the energy harvesting module is enabled in the sensor node, the software will adjust the duty cycle according to the current energy level. The software algorithm for wearable sensor nodes is presented in Fig. 7.

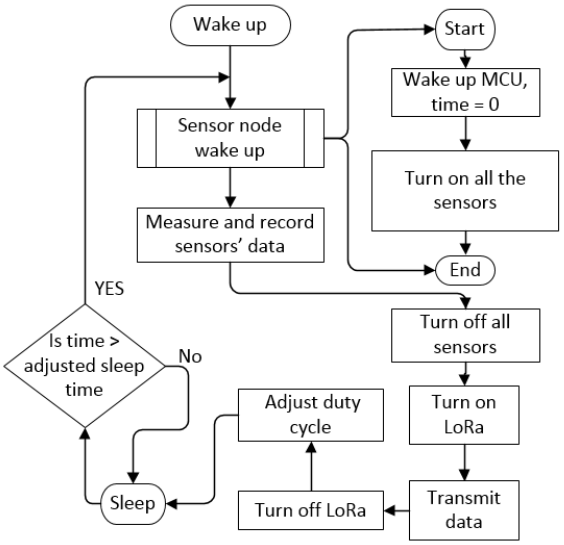

FIGURE 7. The wearable node's software algorithm.

The gateway, a Raspberry Pi Mode 3, receives the data from the wearable sensor nodes. It displays the data in a local Graphical User Interface (GUI) and stores the data into a local MySQL database. The data will ultimately be transmitted to a cloud server.

The networking topology is a star type network. All the data from the wearable sensor nodes is transmitted directly to the gateway node.

IV. EXPERIMENTAL RESULTS AND DISCUSSION

To evaluate the WE-Safe wearable sensor network, a few experiments are conducted and presented in the following sections.

A. PERFORMANCE EVALUATION OF SOLAR ENERGY HARVESTER

Fig. 8 shows the charging characteristics at 600 lux using a 0.1 F super-capacitor with the sensor node disconnected. 0.1 F super-capacitor is used in this experiment because it takes long time to charge 12.5 F super-capacitor, which makes it impractical to monitor the charging and discharging cycle. As shown in Fig. 8, the blue line represents the super-capacitor voltage, and the red line indicates the solar cell voltage. When the energy storage unit voltage is below

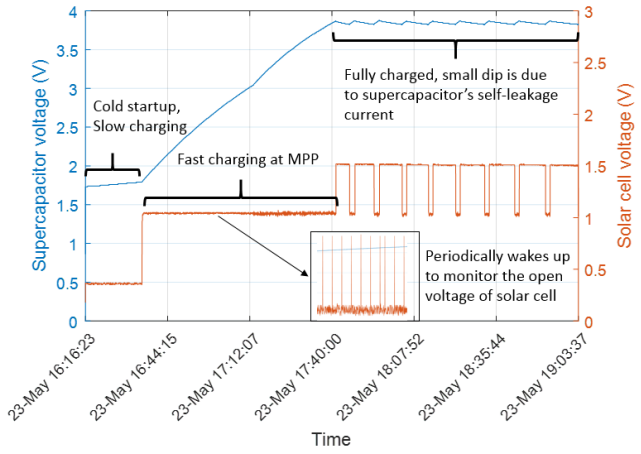

FIGURE 8. Energy harvesting module charging a 0.1 F super-capacitor (indoor, lux 600).

1.93 V (the Cold-Start Operation Threshold), the module is operating in cold-startup mode and the charging rate is relatively slow, which is about 0.78 V/hour. After the cold startup mode finishes, the boost regulator starts charging the super-capacitor at the solar panel's MPP point, and the charging rate increases to approximately 1.83 V/hour.

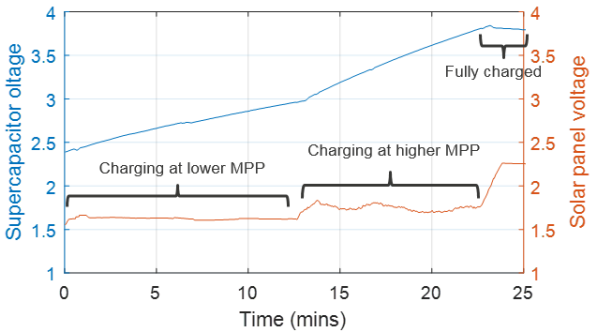

FIGURE 9. The energy harvesting module charging a 12.5 F super-capacitor (outdoor).

The charging rate becomes much higher when the sensor node is placed at outdoor under direct sunlight as shown in Fig. 9. To avoid the slow charging period at cold start-up, the 12.5 F super-capacitor is pre-charged to 2.4 V. The module's charging rate is relatively lower at 0.0445 V/min at the lower MPP point 1.6 V. After 12 minutes the charging rate increases to 0.08 V/min at the higher MPP 1.7 V because the solar radiation is stronger at this time.

B. POWER CONSUMPTION OF THE WE-SAFE NODE

Fig. 10 shows the current waveform of the WE-Safe node. At first, the sensor node is in sleep mode. Secondly, the sensor node wakes up and enters the sense mode to monitor the environment for around 9 seconds. After all the environmental data is collected, the sensor node enters transmission mode, which is followed by idle mode. Finally, the sensor node

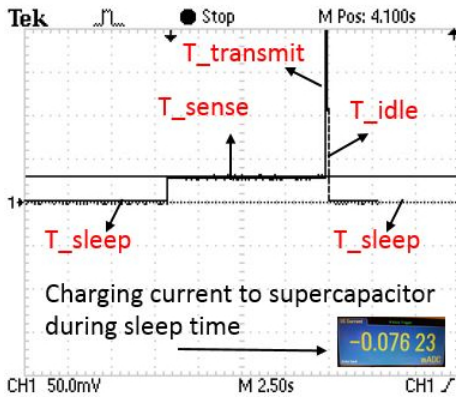

FIGURE 10. The current waveform of the wearable sensor node.

enters sleep mode again in order to save power. During the current waveform testing, the solar panel is connected and the energy harvesting module is functioning. It can be seen from the figure that during sleep time, the solar energy harvester is able to charge the super-capacitor and the charging current is 76.23 μA under indoor ambient light.

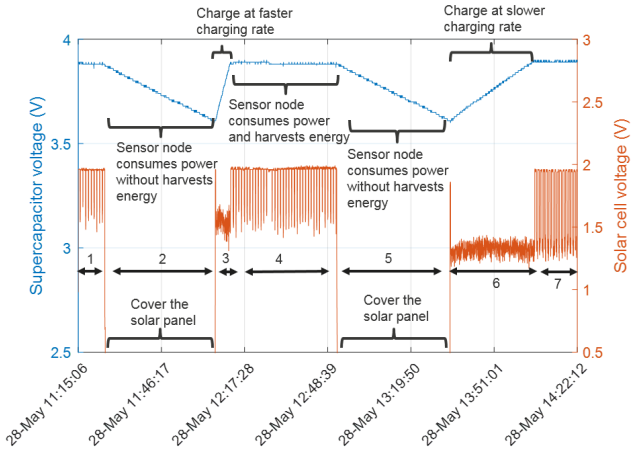

FIGURE 11. The waveform of continuous monitoring the voltage of the super-capacitor and the solar panel while discharging and charging.

Fig. 11 shows the monitoring of the 12.5 F super-capacitor voltage and the solar cell voltage vs time. As can be seen from the figure, the super-capacitor voltage can maintain at 3.8 V during stages 1, 4, and 7. During these three stages, sensor node monitors the environment every minute and harvests the energy at the same time. The harvested energy is sufficient to provide for the sensor node energy consumption. There are some peaks of solar cell voltage, which represents the solar cell's open voltage.

During stages 2 and 5, the solar panel is fully covered and the energy harvester stops charging the super-capacitor. As shown in the figure, the super-capacitor's voltage decreases linearly from 3.9 V to 3.6 V. The discharging rate is 0.00654 V/min. In stages 3 and 6, the energy harvester starts to work again. The solar cell operates at a higher voltage in stage 3 compared to stage 5 and the charging rate is 0.049 V/min in stage 3 and 0.0094 V/min in stage 6.

C. NETWORK PERFORMANCE

The proposed network system has been tested both indoors and outdoors at the Monash University campus. The gateway node is placed inside a laboratory and close to a window on the second floor. The wearable nodes are positioned on the subject's body and moving around the campus.

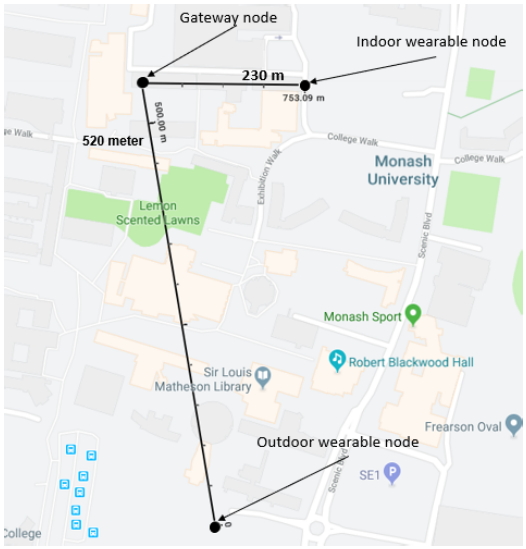

FIGURE 12. Outdoor and indoor coverage of LoRa: urban dense area.

Fig. 12 shows the coverage of the campus LoRa network. At first, outdoor coverage is tested. The wearable node is worn on the subject when walking around the campus, and the data from the LoRa node is transmitted to the gateway node. As shown in Fig. 12, when the wearable node is outdoors, the network can cover up to 520 meters before the signal is lost. This outdoor coverage test is comparable to an dense urban area because there are many building between the wearable node and gateway node. The antenna used in this experiment is a 3 dBi antenna. When the wearable node is indoors, the network can cover up to 230 meters.

D. REAL-TIME MONITORING FOR MOVING SENSOR NODES

Fig. 13 shows an example of a WE-Safe sensor node that is attached to the subject's body. The UV sensor is placed on top of the solar cell. The sensor node's PCB, on-board sensors, and the LoRa module are at the bottom and inside the enclosure. The CO_2 sensor is in the middle. The height of the sensor node is 4.5 cm, which is mainly due to the size of the CO_2 sensor. More compact size can be achieved by using some small-sized environmental sensors and reducing the size the sensor node's printed circuit board.

Fig. 14 shows the real-time monitoring of temperature, relative humidity, UV index and CO_2 concentration from one wearable sensor node as the user moves around the campus.

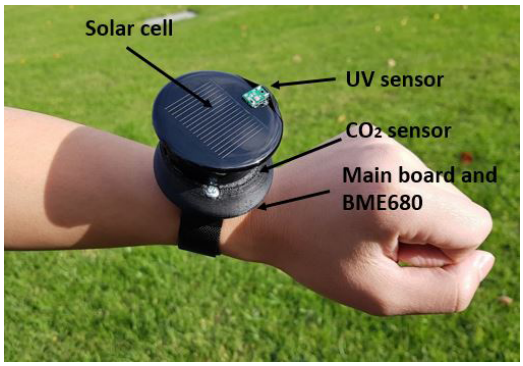

FIGURE 13. The WE-Safe sensor node is attached to the human body.

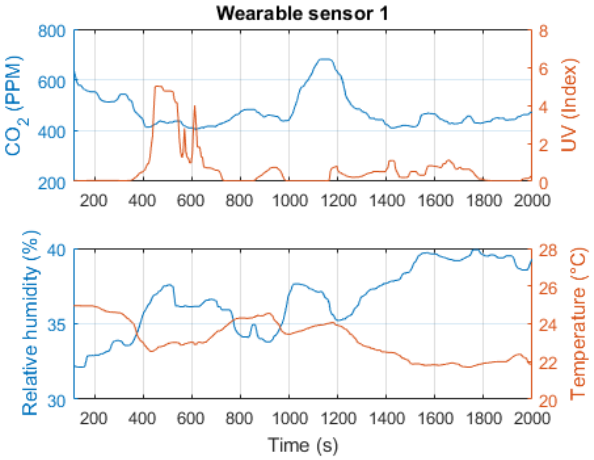

FIGURE 14. Example of data collected from a moving WE-Safe node 1.

From 0 to 200 s, the CO_2 concentration decreases. This is because the user is moving towards outdoor. From 400 TO 700 s, CO_2 remains at approximately 400 to 420 ppm outdoors. During the same period, the UV index is reported to be higher than 4, i.e. when the subject is exposed to sunlight. From 1000 to 1200 s, the CO_2 increases to above 600 ppm, while the uv lower than 1, since the subject is inside an building. This figure also shows that the reading of temperature and relative humidity shows opposite trends. This is expected as an warmer temperature absorbs more moisture, which results in a lower relative humidity.

Fig. 15 shows the real-time monitoring of temperature, relative humidity, and UV index from two wearable sensor nodes as users move around the campus. Two nodes are positioned on both subjects' wrist as shown in Fig.13. Overall, the readings between two wearable nodes are similar and match each other. Two wearable nodes are able to detect changing environments and successfully transmit the data to the gateway. From 1000 to 1200 s, the temperature value of wearable sensor node 1 is slightly higher than wearable sensor node 2. This is because during that time, sensor node 1 was completely exposed to sunlight, while sensor node 2 was only partially exposed. It can be shown from the UV data that from 1000 s to 1200 s, the UV measured by sensor node 1 is higher

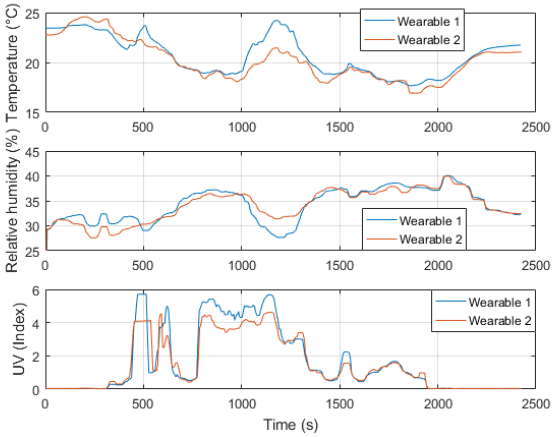

FIGURE 15. Example of data collected from two moving WE-Safe nodes.

than sensor node 2. The same situation happens at around 500 s where the temperature and UV of sensor node 1 is slightly higher than sensor node 2. It is expected that the relative humidity captured by sensor node 1 is slightly lower than sensor node 2 during these periods.

V. CONCLUSION

This paper presents a self-powered wearable IoT sensor network system for safety applications (WE-Safe project). Surrounding environmental data is collected and sent to a remote cloud via the LoRa network. The micro-power manager is able to harvest solar energy from both indoor and outdoor environments to enable a continuous energy supply for the sensor node.

The aim of this paper is to provide an effective and convenient solution for people working in harsh environments. The experimental results show that the system can provide reliable and real-time data. Such an IoT platform will also present new opportunities for preventing health issues especially for people subjected to harsh environments. Currently, the gateway is only used to forward the message from the wearable network to the cloud service. In the future, the work can be improved by by utilizing the gateway to send control messages to wearable sensor nodes in order to control the duty-cycle, transmission data rate, and transmission power according different applications' requirements. The gateway can also enable edge computing to support time-dependent applications, so as to improve the network's reliability and availability.

REFERENCES

[1] S. Wen, H. Heidari, A. Vilouras, and R. Dahiya, "A wearable fabric-based RFID skin temperature monitoring patch," in *Proc. IEEE SENSORS*, Oct. 2016, pp. 1–3. [Online]. Available: http://ieeexplore.ieee.org/document/7808919/

[2] B. Latré, B. Braem, I. Moerman, C. Blondia, and P. Demeester, "A survey on wireless body area networks," *Wireless Netw.*, vol. 17, no. 1, pp. 1–18, 2011.

[3] M. R. Yuce and J. Y. Khan, *Wireless Body Area Networks: Technology, Implementation and Applications*, 2011. [Online]. Available: http://www.scopus.com/inward/record.url?eid=2-s2.0-84881815399&partnerID=tZOtx3y1

[4] T. Wu, F. Wu, J. M. Redouté, and M. R. Yuce, "An autonomous wireless body area network implementation towards IoT connected healthcare applications," *IEEE Access*, vol. 5, pp. 11413–11422, 2017.
[5] D. Antolín, N. Medrano, B. Calvo, and F. Pérez, "A wearable wireless sensor network for indoor smart environment monitoring in safety applications," *Sensors*, vol. 17, no. 2, p. 365, 2017. [Online]. Available: http://www.mdpi.com/1424-8220/17/2/365
[6] E. Wilhelm *et al.*, "Wearable environmental sensors and infrastructure for mobile large-scale urban deployment," *IEEE Sensors J.*, vol. 16, no. 22, pp. 8111–8123, Nov. 2016.
[7] M. Serbanescu, V. M. Placinta, O. E. Hutanu, and C. Ravariu, "Smart, low power, wearable multi-sensor data acquisition system for environmental monitoring," in *Proc. 10th Int. Symp. Adv. Topics Elect. Eng. (ATEE)*, pp. 118–123, 2017.
[8] F. Tsow *et al.*, "A wearable and wireless sensor system for real-time monitoring of toxic environmental volatile organic compounds," *IEEE Sensors J.*, vol. 9, no. 12, pp. 1734–1740, Dec. 2009.
[9] A. Velasco, R. Ferrero, F. Gandino, B. Montrucchio, and M. Rebaudengo, "A mobile and low-cost system for environmental monitoring: A case study," *Sensors*, vol. 16, no. 5, p. 710, 2016. [Online]. Available: http://www.mdpi.com/1424-8220/16/5/710
[10] X. Yue *et al.*, "Development of an indoor photovoltaic energy harvesting module for autonomous sensors in building air quality applications," *IEEE Internet Things J.*, vol. 4, no. 6, pp. 2092–2103, Dec. 2017.
[11] E. M. Compher, M. C. Gupta, W. C. Wilson, and E. I. Madaras, "Solar powered micrometeorite sensors using indoor ambient light for the international space station," *Sol. Energy*, vol. 85, no. 9, pp. 1899–1905, Sep. 2011. [Online]. Available: http://linkinghub.elsevier.com/retrieve/pii/S0038092X11001496
[12] Y. He, X. Cheng, W. Peng, and G. L. Stuber, "A survey of energy harvesting communications: Models and offline optimal policies," *IEEE Commun. Mag.*, vol. 53, no. 6, pp. 79–85, Jun. 2015. [Online]. Available: http://ieeexplore.ieee.org/document/7120021/
[13] F. Wu, C. Rüdiger, and M. R. Yuce, "Real-time performance of a self-powered environmental IoT sensor network system," *Sensors*, vol. 17, no. 2, p. 282, 2017.
[14] F. Wu, C. Rüdiger, J.-M. Redouté, and M. R. Yuce, "A wearable multi-sensor IoT network system for environmental monitoring," in *Proc. BodyNets*. Dalian, China: EAI, 2017, pp. 1–10.
[15] Bosch Sensortec. (2017). *BME680 Low Power Gas, Pressure, Temperature & Humidity Sensor [Datasheet]*. [Online]. Available: https://ae-bst.resource.bosch.com/media/_tech/media/datasheets/BST-BME680-DS001-00.pdf
[16] M-Sensors. *GSS Sensor User's Manual*. Accessed: May 20, 2018. [Online]. Available: http://www.co2meters.com/Documentation/Manuals/Manual-GSS-Sensors.pdf
[17] Silicon Labs. (2014). *Si1145/46/47 Proximity/UV/Ambient Light Sensor IC With I2C Interface [Datesheet]*. [Online]. Available: https://www.silabs.com/documents/public/data-sheets/Si1145-46-47.pdf
[18] M. Bor, J. Vidler, and U. Roedig, "LoRa for the Internet of Things," in *Proc. Int. Conf. Embedded Wireless Syst. Netw.*, 2016, pp. 361–366.
[19] Hope Microelectronics Co. (2014). *RFM95/96/97/98(W) [Datasheet]*. [Online]. Available: http://www.hoperf.com/upload/rf/RFM95_96_97_98W.pdf
[20] Mike McCauley. *RadioHead Packet Radio Library for Embedded Microprocessors*. Accessed: May 20, 2018. [Online]. Available: http://www.airspayce.com/mikem/arduino/RadioHead/
[21] Analog Devices. (2015). *Ultralow Power Boost Regulator with MPPT and Charge Management [Datasheet]*. [Online]. Available: http://www.analog.com/media/en/technical-documentation/data-sheets/ADP5090.pdf
[22] Microchip Technology. (2016). *Ultra-Low Quiescent Current LDO Regulator MCP1810 [Datasheet]*. [Online]. Available: http://ww1.microchip.com/downloads/en/DeviceDoc/20005623A.pdf
[23] Texas Instruments. (2015). *TPS22908 [Datasheet]*. [Online]. Available: http://www.ti.com/lit/ds/symlink/tps22908.pdf

FAN WU (S'17) received the B.E. degree from Monash University in 2015, where he is currently pursuing the Ph.D. degree in electrical and computer systems engineering. From 2015 to 2017, he was a Research Assistant with the Engineering Department. His main areas of research interests are wireless sensor network, wearable sensors, energy harvesting, and IoT innovations.

JEAN-MICHEL REDOUTÉ (M'09–SM'12) received the M.S. degree in electronics from the University College of Antwerp, Belgium, in 1998, the M.Eng. degree in electrical engineering from the University of Brussels, Belgium, in 2001, and the Ph.D. degree entitled "Design of EMI resisting analog integrated circuits" in 2009. In 2001, he was at Alcatel Bell, Antwerp, where he was involved in the design of analog microelectronic circuits for telecommunications systems. In 2005, he joined ESAT-MICAS laboratories, University of Leuven, as a Ph.D. Research Assistant. In 2009, he was at the Berkeley Wireless Research Center, University of California at Berkeley, as a Post-Doctoral Scholar. In 2010, he joined Monash University as a Senior Lecturer. His research interests include mixed-signal integrated circuit design, electromagnetic compatibility, biomedical (integrated and non-integrated) circuit design, and radio-frequency integrated circuit design.

MEHMET RASIT YUCE (S'01–M'05–SM'10) received the M.S. degree in electrical and computer engineering from the University of Florida, Gainesville, FL, USA, in 2001, and the Ph.D. degree in electrical and computer engineering from North Carolina State University, Raleigh, NC, USA, in 2004. He was a Post-Doctoral Researcher with the Electrical Engineering Department, University of California at Santa Cruz, in 2005. He was an Academic Member with the School of Electrical Engineering and Computer Science, University of Newcastle, NSW, Australia, until 2011. In 2011, he joined Monash University. He is currently an Associate Professor with the Department of Electrical and Computer Systems Engineering, Monash University, Australia

His research interests include wearable devices, Internet-of-Things for healthcare, wireless implantable telemetry, wireless body area network, bio-sensors, integrated circuit technology dealing with digital, analog, and radio frequency circuit designs for wireless, biomedical, and RF applications. He has published over 150 technical articles in the above areas. He received the NASA Group Achievement Award for developing an SOI transceiver in 2007. He received the Best Journal Paper Award from the IEEE Microwave Theory and Techniques Society in 2014. He received the Research Excellence Award from the Faculty of Engineering and Built Environment, University of Newcastle, in 2010. He has authored the books, such as the *Wireless Body Area Networks* (2011) and the *Ultra-Wideband and 60 GHz Communications for Biomedical Applications* (2013). He is a Topical Editor for the IEEE Sensors Journal, an Associate Editor-In-Chief for *Sensors*, and the Guest Editor for the IEEE Journal of Biomedical and Health Informatics in 2015.